RSC Advances RSCPublishing

ARTICLE

251 fs Pulse Generation With Nd^{3+}-Doped $Ca_3Gd_2(BO_3)_4$ Disordered Crystal

Cite this: DOI: 10.1039/x0xx00000x

Zhongben Pan, ‡[a] Jie Ma, ‡[b] Honghao Xu,[c] Dingyuan Tang,[d] Huaqiang Cai,*[a] Haohai Yu,[e] Huaijin Zhang,**[e] and Jiyang Wang [e]

Received 00th January 2014,
Accepted 00th January 2014

DOI: 10.1039/x0xx00000x

www.rsc.org/

A diode-pumped passively mode-locked femtosecond $Nd:Ca_3Gd_2(BO_3)_4$ disordered crystal laser has been investigated for the first time, to our knowledge. The passive mode locking of the laser is initiated with a semiconductor saturable absorption mirror (SESAM). Stable mode-locked pulses with 251 fs pulse width, 87 MHz repetition rate, and 37 mW average output power have been demonstrated.

Introduction

In the last few decades, ultrashort pulse lasers have attracted a great deal of attention in the applications of telemetry, arbitrary waveform generation, generation of terahertz radiation, medical surgery, high-temperature plasma generation, seeding of ultrafast amplifiers, etc.[1-5] Among the various ultrashort pulse lasers, four-level Nd^{3+}-doped crystals have proved to be an important laser gain medium at 1 μm wavelength region. The Nd^{3+}-doped lasers generally present a certain advantage because of their true four-level laser operation. They usually own the advantages of conveniently minimized pump thresholds and less constraining temperature effects.[6,7] However, the most commonly available Nd^{3+}-doped crystals generally have narrow fluorescence line widths, limiting their applications in ultrashort pulse generation. To date, the development of various Nd^{3+}-doped single crystal ultrafast lasers has been reported; however, the mode-locked pulse duration is usually on the order of picoseconds. To overcome this limitation of Nd^{3+}-doped crystals, Nd^{3+}-ions was used to dope a glass matrix. Due to its inhomogeneously broadened fluorescence spectrum, Nd^{3+}-doped glass has proved to be one of the most commercially successful materials for producing femtosecond laser gain and be used in the chirped-pulse amplification (CPA) system to generate ultrahigh-peak-power laser.[8,9] However, the totally disordered structure of Nd^{3+}-doped glass generates unpolarized emission and relatively poor thermal properties, which limit its further applications. Among crystals, there is a kind of host materials named as disordered crystals. In their structure, there is a partial replacement of the lattice ions, which induces inhomogeneously broadened spectra as in glass. In addition, their crystal merits may induce the better thermal properties and polarized emission which is in favor of high power ultrafast laser output.

Up to now, many disordered crystals have been investigated, but only a few Nd^{3+}-doped disordered crystals have been reported on that produce femtosecond operation. Crystals, such as Nd:CLNGG, Nd:CLNGG-CNGG, $Nd:SrLaGa_3O_7$, $Nd:BaLaGa_3O_7$, Nd:LGS and $Nd,Y:SrF_2$ which have respectively generated 900, 534, 378, 316, 381, and 332 fs pulses have been described.[10-15] And, especially lately, a 103 fs pulses was obtained with a cubic crystal $Nd,Y:CaF_2$.[16] In recent years, rare-earth ion-doped new borate family, $M_3Re_2(BO_3)_4$ (M=Ca, Sr, Ba; Re=Y, La, Gd) with structure of orthorhombic system, has attracted much attention due to their large fluorescence linewidth and potential to generate polarized ultrafast pulses. The structure of $M_3Re_2(BO_3)_4$ is made of three M-oxygen distorted polyhedrons, and the Re and M ions occupy the three M sites statistically, which generates a disordered structure and causes significant inhomogeneous spectrum broadening.[17] The spectroscopic characteristics and continuous-wave (CW) laser performance of Nd^{3+}-doped $Ca_3Gd_2(BO_3)_4$, $Ca_3La_2(BO_3)_4$, $Sr_3La_2(BO_3)_4$, and $Sr_3Y_2(BO_3)_4$ have been reported in our previous work.[18-21] All of these crystals possess a broad absorption and emission spectrum due to inhomogeneous spectrum broadening and splitting. It has been observed that the fluorescence line width of Nd^{3+}-doped $Ca_3Gd_2(BO_3)_4$ (FWHM=30nm), $Ca_3La_2(BO_3)_4$ (FWHM=25nm), $Sr_3La_2(BO_3)_4$ (FWHM=25nm), and $Sr_3Y_2(BO_3)_4$ (FWHM=30nm) are all comparative to Nd:glass (FWHM=20-30nm), which could support the generation of femtosecond pulses. Additionally, for an orthorhombic crystal, the symmetry of its physical properties is determined by that of the structure based on the Neumann principle. Compared with the cubic crystal (such as $Nd,Y:CaF_2$), the Nd-doped $M_3Re_2(BO_3)_4$ (M=Ca, Sr, Ba; Re=Y, La, Gd) crystal with the structure of orthorhombic also possess the features of linear polarized emission. But so far, no mode-locked lasers have been demonstrated in these crystals. In this letter, we demonstrated, for the first time to the best of our knowledge, the successful operation of a passively mode-locked femtosecond laser using a Nd^{3+}-doped $Ca_3Gd_2(BO_3)_4$ disordered crystal. The mode locking of the laser was initiated and sustained by use of a semiconductor saturable absorber mirror (SESAM). With dispersion compensation through a pair of intracavity prisms, stable continuous-wave (CW) mode locking was successfully achieved in the disordered crystal laser, with pulse duration of 251 fs at a center wavelength of 1061.5 nm. The average output power of the laser was about 37 mW with the repetition rate of ~ 87 MHz. To the best of our knowledge, it is one of the shortest pulse generated from the Nd-doped crystal lasers so far.

Experimental details

The experimental laser setups is shown schematically in Fig. 1. The pump source used in the experiment is a fiber-coupled Laser Diode (LD) with a fiber core diameter of 100 μm and N.A. of 0.22. The laser diode emits at a wavelength of 808 nm. The output beam of the LD was focused onto the $Nd:Ca_3Gd_2(BO_3)_4$ crystal sample with a spot radius of about 40 μm by using a focusing lens with focal length of 80 mm. The $Nd:Ca_3Gd_2(BO_3)_4$ disordered crystal was grown by the Czochralski method. The crystal sample used in this experiment has an Nd-doping concentration of 0.53 at.% and was cut to dimensions with a length of 6 mm and cross section of 3×3 mm^2. It was oriented for E//a polarization in the experiment. Both end faces of the crystal that perpendicular to its *b* direction in crystallographic axes were optically polished and anti-reflection (AR) coated at the lasing wavelength of 1064 nm and at the pumping wavelength of 808 nm. In order to remove the heat generated as a result of pumping, the crystal was wrapped with indium foil and tightly mounted in a water-cooled copper block. The cooling water was maintained at a temperature of 16.5 ℃. A standard X-folded five mirrors cavity was used in the experiment to achieve suitable laser mode sizes in the laser crystal and on the SESAM (BATOP GmBH). The three concave mirrors M1, M2, and M3, had a radius of curvature of 100 mm, 300 mm and 100 mm, respectively. They were all high-reflectivity coated for the laser wavelength (1000-1100 nm) and anti-reflectively coated for the pump wavelength. Three planar wedged output couplers with different transmission of 1.6%, 2.4%, and 3.5% from 1020 nm to 1100 nm were used in the experiment, respectively. In order to achieve femtosecond pulse operation, a pair of SF10 prisms with a tip-to-tip distance of 56 cm was used in the cavity to compensate for dispersion of the resonator. In the experiment, the pair of prism provided the negative dispersion of about –1400 fs^2. Based on the ABCD propagation matrix method, the waist radius of laser mode in the crystal and on the SEASAM were calculated to be about 45 μm and 30 μm, respectively. The pulse trains were detected by a high-speed photoreceiver (New Focus, Model: 1611) together with a 1 GHz digital oscilloscope (Tektronix, DPO7104). The optical spectrum was measured by using an optical spectrum analyzer (Ocean Optics, USB4000) and the pulse width was measured by a commercial autocorrelator (APE, PulseCheck 50).

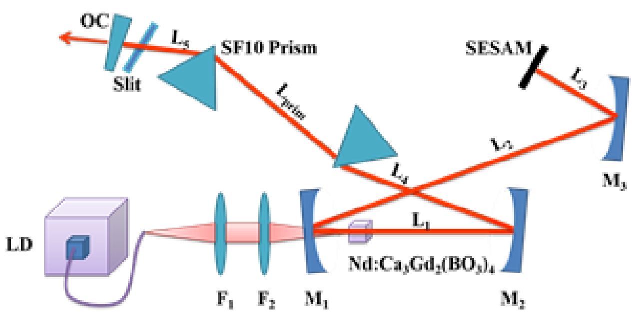

Fig. 1. Schematic of the laser setup. LD, laser diode; F1, F2, lenses with focal length of 100 and 80 mm, respectively; M1, M2 and M3: plano-concave mirrors, ROC—-100 mm, -300 mm, and -100 mm, respectively; L1—23.5 cm, L2—59 cm, L3—5 cm, L4—12.5 cm, L5—16 cm, Lprism—56 cm.

Results and discussion

The disordered crystal usually has a relatively wide absorption and emission spectrum, which could potentially generate ultrashort mode-locked pulses. In order to investigate the potentiality of ultrashort pulse generation of the $Nd:Ca_3Gd_2(BO_3)_4$ disordered crystal, we studied the wavelength tuning performance of it. In the experiment, a standard X-folded five-mirror cavity with an output coupling of 0.8% was employed, as shown in Fig. 1. The SESAM was replaced by a high-reflection plane mirror to reduce total cavity losses. The wavelength tuning was conducted by inserting a slit near the output coupler. And by adjusting the slit, the wavelength tuning could be realized. Fig. 2 shows the tuning spectra and corresponding output power under the pump power of 3.45 W. It can be seen that a wide tuning range of 35 nm from 1054 nm to 1089 nm was obtained in the experiment, showing that $Nd:Ca_3Gd_2(BO_3)_4$ is a very promising crystal for femtosecond pulse generation by mode-locking.

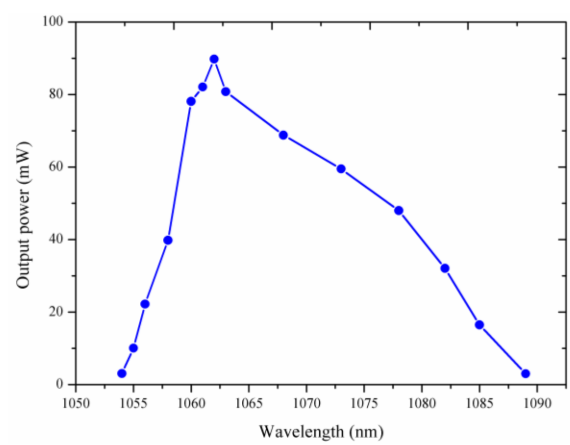

Fig. 2. Wavelength tuning trace of the $Nd:Ca_3Gd_2(BO_3)_4$ laser.

By using the laser setup shown in Fig. 1, mode-locked operation of the laser was obtained in the experiment. A commercial SESAM with a modulation depth of 1.2% and a relaxation time of 1 ps was used in the experiment. And to investigate the performances of mode-locked laser, three output couplers with different transmission of 1.6%, 2.4%, and 3.5% were used. As shown in Fig. 3, the maximum output power of 37.0 mW, 45.1 mW and 45.4 mW were obtained under an absorbed pump power of 1.72 W, corresponding to the slope efficiency of 3.7%, 4.2% and 7.5%, respectively. The maximum average output power was 45.4 mW at an absorbed pump power of 1.72 W by using the 3.5% output coupler. When we further increased the pump power, the mode-locking became unstable. It can be found that the laser threshold for 3.5% OC is higher because the large output coupler means large losses for laser cavity. And for mode-locked laser, the output power usually becomes higher obviously when the operation regime changes from CW to CW mode locking. That is because the intracavity losses became weaker. So we could observe obvious changes of output power for 3.5% output coupler at the different laser operation regimes. In the experiment, the mode-locked pulses were monitored by a high-speed photoreceiver and displayed on a digital oscilloscope with a 1GHz bandwidth. Fig. 4 shows the typical mode-locked pulse trains of the laser in nanosecond and millisecond timescales. It can be found that the mode-locking was very stable, no Q-switching signal was observed. The radio-frequency (RF) spectrum of the mode-locked laser was also measured in the experiment, as shown in Fig. 5. The RF spectrum shows a high signal-to-noise ratio of about 73 dB around the fundamental frequency at a resolution bandwidth of 1 kHz and a 400 kHz span, which is a further evidence for stable CW mode locking without Q-switching. The pulse repetition rate is about 87 MHz, corresponding to the laser cavity length of ~ 1.72 m.

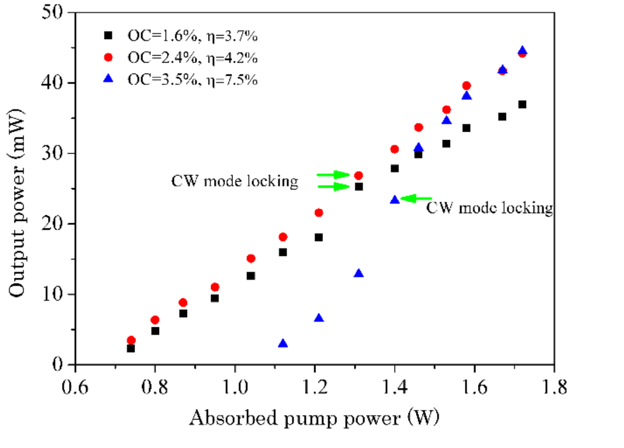

Fig. 3. Average output power versus absorbed pump power of the mode-locked laser using three different output couplers.

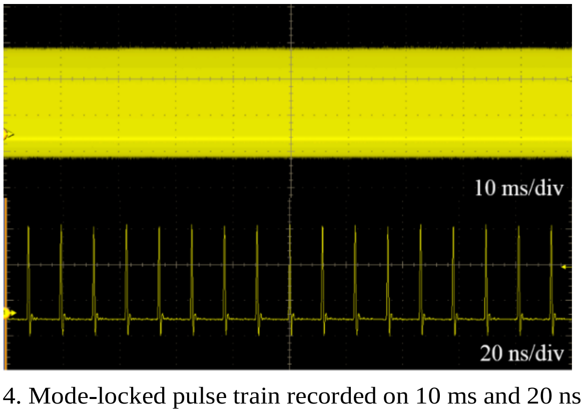

Fig. 4. Mode-locked pulse train recorded on 10 ms and 20 ns per division time scales.

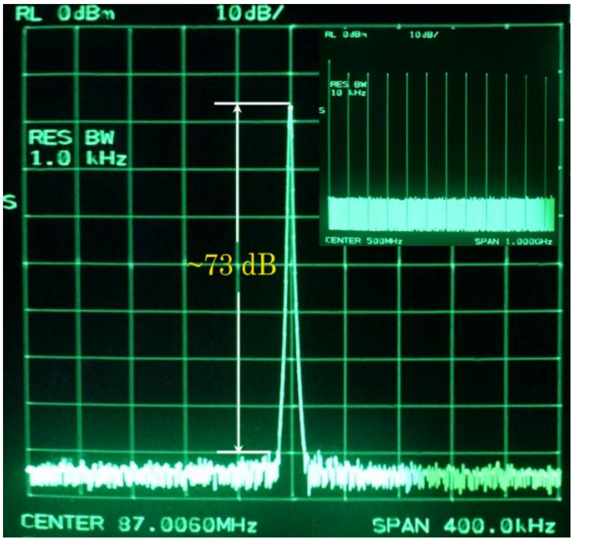

Fig. 5. RF spectrum of the laser output. Insert: RF spectrum up to 1 GHz.

By using the output coupler with transmission of 1.6%, the shortest mode-locked pulses were achieved in the experiment. Fig. 6 shows the autocorrelation trace of the mode-locked laser pulses with 1.6% output coupler. The autocorrelation trace obtained from a commercial autocorrelator (APE, PulseCheck 50) is well fitted assuming a sech^2-pulse shape with the full width at half maximum (FWHM) of about 386 fs, corresponding to the pulse duration of 251 fs. The corresponding spectrum of the mode-locked pulses is shown in the right inset of Fig. 6. The mode-locked pulse spectrum is measured by an optical spectrometer (Ocean Optics, USB4000) with a resolution of 1.0 nm. The spectrum is centered at 1061.5 nm with an FWHM bandwidth of ~ 5.8 nm. The time-bandwidth product is calculated to be ~ 0.38, a value that is very close to the Fourier-transform limit of 0.315 for sech2 shaped pulses.

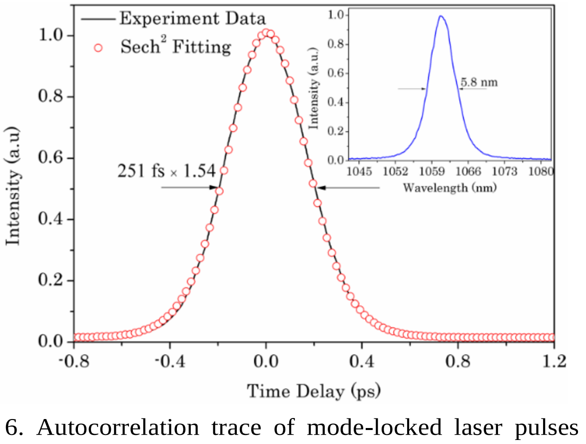

Fig. 6. Autocorrelation trace of mode-locked laser pulses by using 1.6% output coupler. Inset: Spectrum of mode-locked laser pulses with a spectrum FWHM of 5.8 nm at central wavelength of 1061.5 nm.

Figure 7 and Fig. 8 show the autocorrelation traces by using the other two output couplers with transmission of 2.4% and 3.5%. Assuming a sech^2-pulse shape, the mode-locked pulse duration of 285 fs and 486 fs were obtained in the experiment. The mode-locked spectra both centered at 1061.5 nm with

FWHM bandwidth of ~ 5.1 nm and ~ 3.5 nm, respectively. The corresponding time-bandwidth products of the mode-locked pulses were about 0.38 and 0.40, which were both close to the Fourier-transform limit for $sech^2$ shaped pulses.

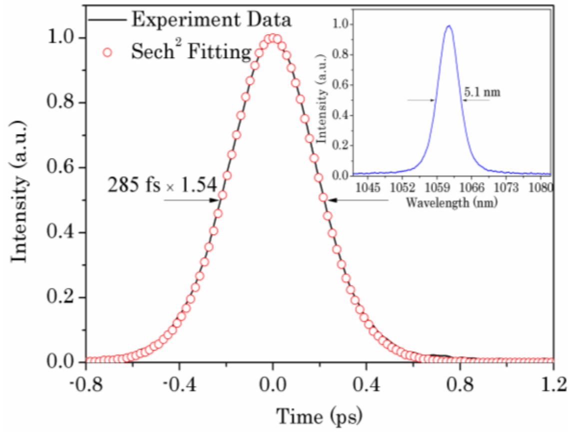

Fig. 7. Autocorrelation trace of mode-locked laser pulses by using 2.4% output coupler. Inset: Spectrum of mode-locked laser with a spectrum FWHM of 5.1 nm at central wavelength of 1061.5 nm

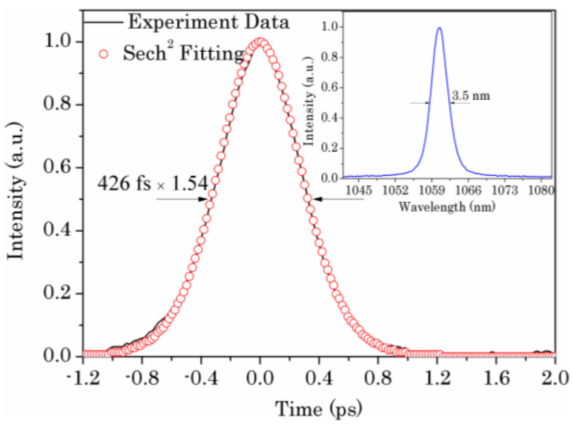

Fig. 8. Autocorrelation trace of mode-locked laser pulses by using 3.5% output coupler. Inset: Spectrum of mode-locked laser with a spectrum FWHM of 3.5 nm at central wavelength of 1061.5 nm

Conclusions

We have demonstrated femtosecond pulse generation with a $Nd:Ca_3Gd_2(BO_3)_4$ disordered crystal. Pumping at 808 nm with a fiber-coupled LD, we obtained mode-locked laser pulses as short as 251 fs with a 37 mW average output power centered at 1061.5 nm. The experiment results indicate that the four-level $Nd:Ca_3Gd_2(BO_3)_4$ disordered crystal is a very promising candidate for the generation of femtosecond laser pulses at 1 μm wavelength region.

Acknowledgements

This work is supported by Innovative Cooperation Fund of China Academy of Engineering Physics, China (Nos. kjcx-201202, 201203), the National Natural Science Foundation of China (Grant Nos. 51025210, 51021062, 51402268 and 51422205) and Key Laboratory of Functional Crystals and Laser Technology , TIPC, Chinese Academy of Sciences. And, the author would like to thanks Prof. Boughton of Bowling Green State University for linguistic polish.

Notes and references

[a]Key Laboratory of Science and Technology on High Energy Laser, Institute of Chemical Materials and Advanced Materials Center, China Academy of Engineering Physics, Mianyang 621900, China. E-mail:danluxiusan@126.com
[b]Department of Chemistry and Graphene Research Centre, National University of Singapore, Singapore 117543, Singapore
[c]College of Physics, Qingdao University, Qingdao 266071, China
[d]School of Electrical and Electronic Engineering, Nanyang Technological University, 639798, Singapore
[e]State Key Laboratory of Crystal Materials and Institute of Crystal Materials, Shandong University, Jinan 250100, China. E-mail:huaijinzhang@sdu.edu.cn
‡ Zhongben Pan and Jie Ma contributed equally to this work.

1 U. Keller, *Nature*, 2003, **424**, 831-838.
2 T. T. Basiev, N. A. Es'kov, A. Ya. Karasik, V. V. Osiko, A. A. Sobol, S. N. Ushakov, and M. Helbig, *Opt. Lett.*, 1992, **17**, 201-203.
3 S. T. Cundiff, A. M. Weiner, *Nat. Photonics*, 2010, **4**, 760-766.
4 G. Q. Xie, D. Y. Tang, H. Luo, H. J. Zhang, H. H. Yu, J. Y. Wang, X. T. Tao, M. H. Jiang, and L. J. Qian, *Opt. Lett.*, 2008, **33**, 1872-1874.
5 W. Sibbett, A. A. Lagatsky, and C. T. A. Brown, *Opt. Express*, 2012, **20**, 6989-7001.
6 L. B. Su, Q. G. Wang, H. J. Li, G. Brasse, P. Camy, J. L. Doualan, A. Braud, R. Moncorgé, Y. Y. Zhan, L. H. Zheng, X. B. Qian, and J. Xu, *Laser. Phys. Lett.*, 2013, **10**, 035804.
7 A. Pugžlys, G. Andriukaitis, D. Sidorov, A. Irshad, A. Baltuška, W. J. Lai, P. B. Phua, L. Su, J. Xu, H. Li, R. Li, S. Ališauskas, A. Marcinkevičius, M. E. Fermann, L. Giniūnas, and R. Danielius, *Appl. Phys. B*, 2009, **97**, 339-350.
8 J. A. D. Au, D. K. F. Morier-Genoud, M. Moser, and U. Keller, *Opt. Lett.*, 1997, **22**, 307-309.
9 A. Agnesi, A. Greborio, F. Pirzio, and G. Reali, *Opt. Express*, 2010, **18**, 10098-10103.
10 G. Q. Xie, D. Y. Tang, W. D. Tan, H Luo, H. J. Zhang, H. H. Yu, and J. Y. Wang, *Opt. Lett.*, 2009, **34**, 103-105.
11 G. Q. Xie, L. J. Qian, P. Yuan, D. Y. Tang, W. D. Tan, H. H. Yu, H. J. Zhang, and J. Y. Wang, *Laser Phys. Lett.*, 2010, **7**, 483-486.
12 A. Agnesi, F. Pirzio, L. Tartara, E. Ugolotti, H. Zhang, J. Wang, H. Yu, and V. Petrov, *Laser Phys. Lett.*, 2013, **10**, 105815.
13 A. Agnesi, F. Pirzio, L. Tartara, E. Ugolotti, H. Zhang, J. Wang, H. Yu, V. Petrov, *Laser Phys. Lett.*, 2014, **11**, 035802.
14 J. X. Liu, Z. H. Wang, K. He, L. Wei, Z. G. Zhang, Z. Y. Wei, H. H. Yu, H. J. Zhang, and J. Y. Wang, *Opt. Express*, 2014, **22**, 26933-26938.
15 L. Wei, H. N. Han, W. L. Tian, J. X. Liu, Z. H. Wang, Z. Zhu, Y. L. Jia, L. B. Su, J. Xu, and Z. Y. Wei, *Appl. Phys. Express*, 2014, **7**, 092704.

16 Z. P. Qin, G. Q. Xie, J. Ma, W. Y. Ge, P. Yuan, L. J. Qian, L. B. Su, D. P. Jiang, F. K. Ma, Q. Zhang, Y. X. Gao, and J. Xu, *Opt. Lett.*, 2014, **39**, 1737-1739.
17 Y. Wang, C. Y. Tu, C. C. H, and Z. Y. You, *J. Mater. Res.*, 2004, **19**, 1203-1207.
18 Z. B. Pan, H. J. Zhang, H. H. Yu, M. Xu, Y. Y. Zhang, S. Q. Sun, J. Y. Wang, Q. Wang, Z. Y. Wei and Z. G. Zhang, *Appl. Phys. B.*, 2012, **106**, 197-209.
19 Z. B. Pan, H. J. Cong, H. H. Yu, L. Tian, H. Yuan, H. Q. Cai, H. J. Zhang, H. Huang, J.Y. Wang, Q. Wang, Z. Y. Wei, and Z. G. Zhang, *Opt. Express*, 2013, **21**, 6091-6100.
20 Z. B. Pan, H. Q. Cai, H. Huang, H. H. Yu, H. J. Zhang, and J. Y. Wang, *J. Alloys Compd.*, 2014, **607**, 16-22.
21 Z. B. Pan, H. H. Yu, H. J. Cong, H. J. Zhang, J. Y. Wang, Q. Wang, Z. Y. Wei, Z. G. Zhang, and R. I. Boughton, *Appl. Opt.*, 2012, **51**, 7144-7149.

Table of contents entry

Autocorrelation trace and spectrum of the mode-locked pulses.